
Integrating Planning and Deep Reinforcement Learning via Automatic Induction of Task Substructures

Jung-Chun Liu Chi-Hsien Chang Shao-Hua Sun Tian-Li Yu
National Taiwan University
Taipei, Taiwan
{r10921043, d07921004, shaohuas, tianliyu}@ntu.edu.tw

Abstract

Despite recent advancements, deep reinforcement learning (DRL) still struggles at learning sparse-reward goal-directed tasks, while classical planning excels at addressing hierarchical tasks, yet most of the methods rely on assumptions about pre-defined subtasks. To bridge the best of both worlds, we propose a framework that integrates DRL with classical planning by automatically inducing task structures and substructures from a few demonstrations. Specifically, we adopt abstraction mapping formulation and define critical actions that lead to the transition at the abstraction level. The framework induces critical action schemata regarded as subtasks to solve the problems. Symbolic regression is used for substructure induction by employing genetic programming where the program model reflects prior domain knowledge of effect rules. We compare the proposed framework to state-of-the-art DRL algorithms, imitation learning methods, and an exploration approach in various domains. Experimental results on various tasks show that our proposed framework outperforms all the abovementioned algorithms in terms of sample efficiency and task performance. Moreover, our framework achieves strong generalization performance by effectively inducing new rules and composing task structures. Ablation studies justify the design of our induction module and the proposed genetic programming procedure.

1 Introduction

Deep reinforcement learning (DRL) as an inductive learning method allows agents to deal with high-dimensional decision-making problems considered intractable in the past [4]. DRL has applied to various fields, including robotics [39], autonomous driving [23], and video games [36]. However, exploring complex tasks with sparse and delayed rewards still remains challenging, leading to inapplicability on many real-world problems comprising multiple subtasks, *e.g.*, cooking and furniture assembly.

In contrast, classical planning is a deductive learning method that aims to solve planning and scheduling problems. Particularly, classical planning is adept at finding the sequence of actions in deterministic and known environments. Researchers in classical planning have developed effective planners that can handle large-scale problems [58]. Yet, classical planning agents face difficulties exploring environments due to limitations in model and domain-specific representation in unknown environments where action models are undiscovered.

Several methods work on combining planning and DRL to address hierarchical tasks with high-level abstraction. Konidaris et al. [24] develop a skill-up approach to build a planning representation from skill level to abstract level, while they do not encompass skill acquisition from low-level execu-

tion. Mao et al. [35] introduce an extension of planning domain definition language (PDDL) [16, 48] to model the skill, and Silver et al. [49] propose a method for learning parameterized policies integrated with symbolic operators and neural samplers. However, they consider object-centric representations, which require fully observable environments and carefully designed predicates.

In this paper, we combine classical planning and DRL to augment agents effectively to adapt to environments by inducing underlying prior knowledge from demonstrations. Specifically, we devise a method that induces symbolic knowledge using genetic programming [25], an evolutionary computation approach, to discover task substructures represented as expression trees that accurately capture the underlying patterns within the data. The compositional property of the programs enables generalizability that adapts to new environments by discovering new substructures from known ones.

To evaluate the proposed framework, we design three gridworld environments where agents can move on and interact with objects. The results show the improvement of DRL agents and outperformance compared to other imitation learning and exploration-based methods. Also, our framework demonstrates generalizability by inducing variant substructures and recomposing task structures. Finally, we show the ablation studies about the efficacy of the induction module.

2 Related Work

Learning abstraction from demonstrations. State abstraction facilitates the agent’s reasoning capabilities in high-level planning by extracting symbolic representations from low-level states [1, 17]. Agents can learn the abstraction from demonstrations since demonstrations encompass valuable information regarding task composition and relevant features [7]. Some methods were developed to extract task decomposition and abstraction from demonstrations [18, 11]. Our work extends these approaches to infer knowledge from demonstrations.

Learning planning action models. Some works have focused on integrating learning and planning to enhance capabilities in complex environments [12, 59]. To leverage the strategies of classical planning, many works have developed building planning action models, including skill acquisition and action schema learning [3, 53, 40, 9, 49, 35, 64]. However, these works mainly focus on the existing planning benchmark and less focus on general Markov decision process (MDP) problems. On the other hand, to address the issue of sample efficiency in DRL, several techniques explored the integration of symbolic knowledge with DRL by learning planning action models [22, 34]. In this work, we aim to bridge this gap by extending these approaches to incorporate inferred knowledge into DRL, enhancing its applicability in complex decision-making scenarios.

Hierarchical task learning. A proper hierarchical structure is crucial for task decomposition and abstraction. Various methods have been proposed for constructing hierarchical task representation [41], including graphs [56], automata [15, 20, 21, 63], programs [54, 55, 57, 32, 29], and hierarchical task networks [18, 51, 28]. Some approaches utilize the capabilities of deep learning with intrinsic rewards [26, 13]. In addition, some of these works specifically address leveraging knowledge to deal with multiple compositional tasks via task decomposition [2, 52, 31, 55, 50, 15]. Despite the success in building hierarchical models shown in previous works, these works put less emphasis on inducing subtask rules and substructure. Therefore, we develop a method to induce symbolic knowledge and leverage it for hierarchical task representation.

3 Problem Formulation

We address the sparse-reward goal-directed problems which can be formulated as MDPs denoted as $\langle \mathcal{S}, \mathcal{A}, T, R, \gamma \rangle$, where \mathcal{S} denotes state space, \mathcal{A} denotes action space, $T : \mathcal{S} \times \mathcal{A} \rightarrow \mathcal{S}$ denotes a transition function, $R : \mathcal{S} \times \mathcal{A} \rightarrow \mathbb{R}$ denotes a reward function, and $\gamma \in (0, 1]$ denotes a discounting factor. DRL agents often struggle at solving sparse-reward, hierarchical tasks, while classical planning techniques excel in such scenarios. On the other hand, unlike classical planning, DRL is regarded as a generic model-free framework that does not require pre-defined models. This motivates us to bridge the best of both worlds by integrating these two paradigms.

However, while DRL directly learns from interacting with MDPs and represents the action and the states with fixed vectors of numeric values, classical planning operates on literal conjunctions. To

address this gap, we integrate planning and DRL methods by annotating the specific MDP actions in the form of action schemata. Specifically, we consider the problem of inducing the action schemata from the near-optimal demonstrations which may exhibit deviations from the optimal solutions. The objective is to induce the action schemata which can be leveraged for task structure deduction. After the action schemata are discovered, the framework deduces task structures from the action model and aims to offer guidance for the training of DRL agents based on the task structures.

4 Integration of MDP in DRL and Planning with Critical Action

To bridge the gap between DRL and planning, we introduce the concept of critical actions in this section. Specifically, we formulate our problems as mapping tasks described by MDPs to PDDL and SAS⁺ [8], where the preliminary notation is elaborated in Appendix A. To express numeric variables, we adopt the configuration of PDDL 2.1 [14], which includes arithmetic operators for specification.

Mapping between MDP and classical planning. Lee et al. [27] has developed the abstraction mapping between planning and MDP problems. A planning task $\Pi = \langle \mathcal{V}, \mathcal{O}, s'_g \rangle$, where \mathcal{V} is a set of variables, \mathcal{O} is a set of operators in the domain, and s'_g is a partial state describing the goal. The transition graph of the planning task is a tuple $\mathcal{T}' = \langle \mathcal{S}', \mathcal{T}', \mathcal{S}'_{goal} \rangle$, where \mathcal{T}' is a set of transitions $\langle s', o, T'(s') \rangle$ for all $s' \in \mathcal{S}'$, and \mathcal{S}'_{goal} is a set of goal states. Let $\mathcal{L} : \mathcal{S} \rightarrow \mathcal{S}'$ be a mapping from the MDP state space \mathcal{S} to high-level planning state space \mathcal{S}' . Given an MDP problem, the abstraction $\langle \mathcal{L}, \Pi \rangle$ is proper iff there exists a mapping \mathcal{L} to Π such that $\langle \mathcal{L}(s), \psi, \mathcal{L}(T(s, a_\psi)) \rangle \in \mathcal{T}'$ if some ψ is admissible in the MDP state $s \in \mathcal{S}$ or $\mathcal{L}(s) = \mathcal{L}(T(s, a_\psi))$, where \mathcal{T}' is a set of all possible transitions in Π . In this work, we focus on the MDP problems with proper abstraction in which a mapping to a planning domain exists, and action models can be induced by the proposed framework.

Critical action. Critical actions are the actions which lead to the transitions in \mathcal{T}' . That is, these actions are critical for progress at the planning level and must be executed in a specific order. A state $s' \in \mathcal{S}'$ in the planning domain is an assignment to \mathcal{V} , and $s'_v \in \mathbb{R}$ is the value assigned to the variable $v \in \mathcal{V}$. We map each s_i in MDP problems with distinct s'_v in planning, considering a planning task as an MDP-like tuple $\langle \mathcal{S}', \mathcal{O}, \mathcal{T}' \rangle$, a transition $\langle s, a_\psi, T(s, a_\psi) \rangle$ in an MDP problem can be directly transferred to the transition $\langle \mathcal{L}(s), \psi, \mathcal{L}(T(s, a_\psi)) \rangle$ in planning domain.

The critical actions can be recognized from the effects which are necessary state changes to achieve a goal. Thus, we define critical action schemata with the critical effects and the required preconditions in classical planning, considering mapping the problem to a planning task Π . A critical action $\psi \in \mathcal{O}$ is a planning operator whose action schema can be defined as a tuple $\langle a_\psi, pre(\psi), eff(\psi) \rangle$. We define the notations as follows, and an illustration is shown in Figure 1.

- **MDP action** $a_\psi \in \mathcal{A}$ denotes the MDP action mapping to ψ .
- **Precondition** $pre(\psi)$ is a set of conditions requires satisfaction before executing ψ .
- **Effect** $eff(\psi)$ is a set of functions which indicates the state change after executing ψ .

Given an effect $eff(\psi)$ and one of its variables $v \in \mathcal{V}(eff(\psi))$, an effect rule $eff(\psi)_v : \mathbb{R} \rightarrow \mathbb{R}$ is a function which transfers the specific feature value s'_v in s' to another value $eff(\psi)_v[s'_v]$ in the transition, and a precondition rule $pre(\psi)_v$ is a logical formula $pre(\psi)_v : \mathbb{R} \rightarrow \{0, 1\}$ that determines whether the variable v is satisfied to execute ψ . Given a state s' , two critical action ψ and ϕ , $eff(\psi)_v$ satisfy $pre(\phi)_v$ in state s' iff a variable v in both $\mathcal{V}(eff(\psi))$ and $\mathcal{V}(pre(\phi))$, and $pre(\phi)_v[s'_v]$ is false while $pre(\phi)_v[eff(\psi)_v[s'_v]]$ is true in a transition with ψ . That is, executing ψ makes ϕ become admissible.

To efficiently induce the model, we assume that the properties of the features in a state are known. Effect variable space $\mathbb{E} = \{v \mid v \in \mathcal{V}(eff(\psi)) \forall \psi \in \mathcal{O}\}$ contains the variables that will change in transitions and related to the progress of the tasks.

Critical-action network. This work represents symbolic knowledge structures as critical-action networks illustrated in Figure 1c. Given a set of critical actions \mathcal{O} and a desired goal specification p_{goal} , a critical-action network $\mathcal{G} = (V, E)$ is an in-tree structure where the root is the critical action

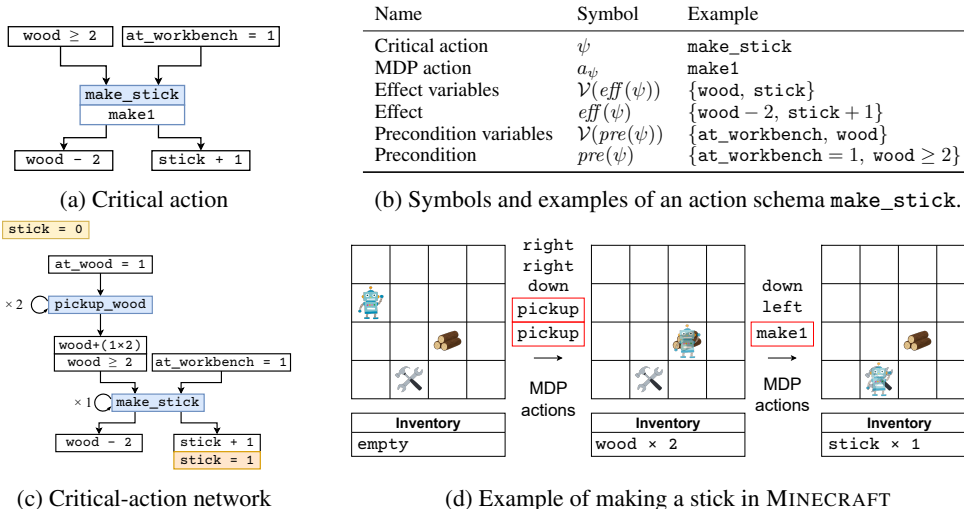


Figure 1: **Critical action.** (a)-(b) The illustration, symbols, and examples of a critical action. A critical action is an essential action in environments with preconditions and effects. (c) **Critical-action network.** If an action model is discovered by the induction module, it builds critical-action networks. (d) **Example of making a stick in MINECRAFT.** Actions highlighted by red rectangles are critical, *i.e.*, picking up wood twice and making a stick (make1).

that can satisfy the goal specification directly. For each edge $(\psi, \phi) \in E$, there exists $eff(\psi)_v$ for some v that satisfy $pre(\phi)_v$. Once the action schemata are known, we can construct the network using planners or backward chaining.

5 Method

Section 5.1 introduces the induction module that determines the critical actions from near-optimal demonstrations and extracts symbolic rules. Section 5.2 describes the training module that deduces task structures to build critical-action networks online from the given goal. The network contains subtask dependencies, providing guidance through intrinsic rewards and augmenting the training efficiency of DRL agents. An overview of our proposed framework is illustrated in Figure 2a.

5.1 Induction Module

The procedure of the induction module is illustrated in Figure 2b. The module first extracts action-effect linkages $(a, \mathcal{V}(eff(\psi)))$ from demonstrations. Second, the module induces effect rules $eff(\psi)$ given $(a, \mathcal{V}(eff(\psi)))$. Finally, the module leverages the rules to determine the precondition rules $pre(\psi)$ for each $(a, eff(\psi))$. After these steps, the components of critical action schemata are all determined. Note that we name the critical action ψ for the convenience of reference, which is not known when inducing action schemata. We use “.” to represent an undefined critical action. The following paragraphs will elaborate on the details of the induction methods.

Action-effect linkages. Based on the outcome assumption that one action only impacts specific state features, we can detect co-occurrence of what effects often occur after executing a by calculating mutual information [47] between actions and effect variables. Let \mathcal{E} be a set of possible effect variable combinations $\mathcal{V}(eff(\cdot))$ in the transitions of demonstrations. The mutual information $M_{(a, \mathcal{V}(eff(\cdot)))}$ is defined as follows:

$$M_{(a, \mathcal{V}(eff(\cdot)))} = \sum_{a \in \mathcal{A}} \sum_{\mathcal{V}(eff(\cdot)) \in \mathcal{E}} P_{\mathcal{A}\mathcal{E}}(a, \mathcal{V}(eff(\cdot))) \log \frac{P_{\mathcal{A}\mathcal{E}}(a, \mathcal{V}(eff(\cdot)))}{P_{\mathcal{A}}(a)P_{\mathcal{E}}(\mathcal{V}(eff(\cdot)))}, \quad (1)$$

where $P_{\mathcal{A}}(a)$ is the count of transitions with action a ; $P_{\mathcal{E}}(\mathcal{V}(eff(\cdot)))$ is the count of transitions that include variables in $\mathcal{V}(eff(\cdot))$; $P_{\mathcal{A}\mathcal{E}}(a, \mathcal{V}(eff(\cdot)))$ is the count of transitions that include changed

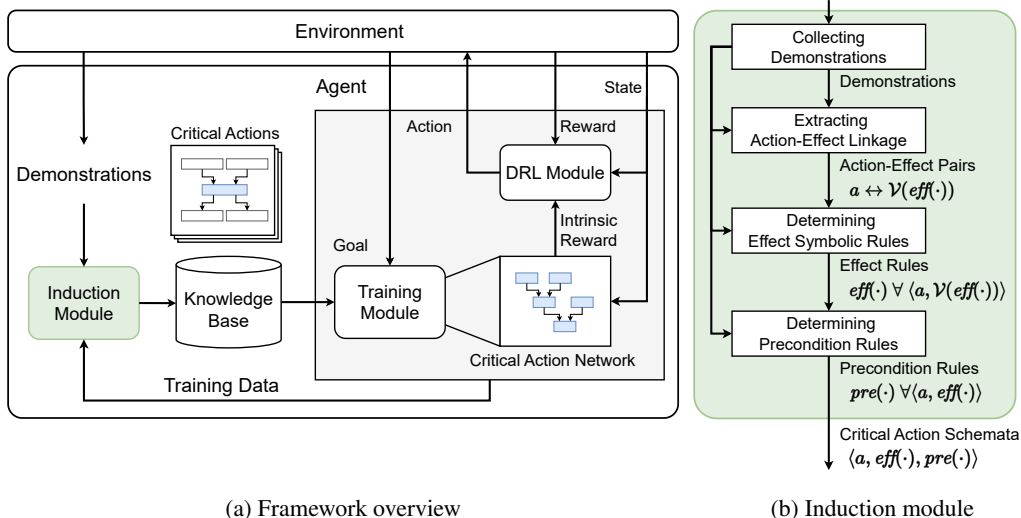


Figure 2: **(a) Framework overview.** The proposed framework is two-stage. In the *induction stage*, critical action schemata are induced from demonstrations. In the *training stage*, the training module deduces the critical-action network from the goal by backward-chaining and offers intrinsic rewards to the DRL module according to the network. **(b) Induction module.** The induction module induces the critical action schemata from demonstrations through three steps. First, it finds the linkage between actions and effect variables in transitions. Then, given the transitions with action-effect linkage, the induction module induces the effect rules via symbolic regression. Finally, it determines the precondition given the specific action and the effect.

variables in $\mathcal{V}(eff(\cdot))$ with action a . To determine the linkage, the pairs are divided into two clusters with the threshold of a maximum gap, and the cluster with higher values are selected. The detailed algorithm is shown in Appendix B.1.

Effect symbolic rules. Given an action-effect pair $(a, \mathcal{V}(eff(\cdot)))$, the induction module proceeds to search for the effect $eff(\cdot)$, which can be formulated as a symbolic regression. To accomplish this, we employ genetic programming for symbolic regression to discover each effect rule $eff(\cdot)_v$ for all v in $\mathcal{V}(eff(\cdot))$, aiming to discover programs that can accurately predict the effects.

In genetic programming, each program is represented as an expression tree, taking s_v and a_ψ in each transition as input and yielding the predicted value of v after the transition as output. The algorithm consists of three key steps: initialization, evaluation, selection, and reproduction. Initially, a population of programs is randomly generated. The fitness of each program is evaluated based on its prediction accuracy, and the programs with the highest fitness values are selected, serving as parents to reproduce offspring through crossover, mutation, and duplication mechanisms. The procedures and the example of genetic programming are illustrated in Figure 3.

The model of symbolic rules is regarded as the substructures of the subtasks, and selecting the proper operators for the symbolic model compatible with the effects plays a crucial role in facilitating effective inference. For instance, in the context of general DRL task with numerical variable representation configuration, arithmetic operation set $\mathcal{F} = \{+, -, \times, \div, inc, dec\}$ is used as the function set in genetic programming, where *inc* denotes an increment operator and *dec* denotes a decrement operator. This choice of function set is consistent with the numerical variable representation commonly employed in DRL tasks. The underlying assumption guiding our approach is that the effects can be expressed through these programs, serving as prior knowledge of the problem. This allows our method to induce task substructures and generalize the knowledge across domains that share identical operation configurations. This distinguishing feature sets our approach apart from alternative model-free methodologies. Additional implementation details can be found in Appendix B.2.

Precondition rules. After the relation between a and $eff(\cdot)$ are found, determining precondition rules $pre(\cdot)$ can be formulated as a classification problem, as the objective is to identify whether $eff(\cdot)$ occurs given the action and the state. The process involves minimal consistent determina-

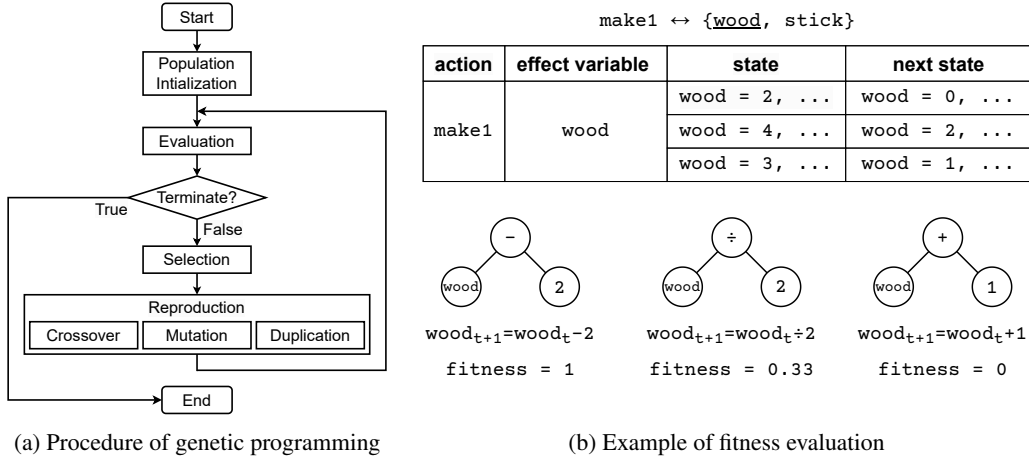


Figure 3: **Symbolic regression using genetic programming.** Given a pair of an MDP action and effect variables, symbolic regression is used to determine the rules when executing the action. **(a) Procedure of genetic programming.** The programs iteratively evolve through fitness evaluation, selection, and reproduction. **(b) Example of fitness evaluation.** The algorithm evaluates the accuracy of programs to induce the rule between make1 and wood.

tion (MCD) and the decision tree method. The model of $pre(\cdot)$ decides what preconditions leading to desired effects after executing a . Additional details can be found in Appendix B.3.

5.2 Training Module

After the induction process, the critical action schemata serve as the components of the knowledge base that guides the agent in the training stage. During the training stage, the training module deduces the critical-action network given the initial state and goal specification and provides intrinsic reward if the agent successfully performs an action that meets the critical effects in the network.

Inferring critical-action network. Once the critical actions schemata are defined, we can infer task structures from the model. Given a goal and an initial state, the proposed framework deduces the critical-action networks by backward chaining. Starting from the goal, the module searches for the critical action to find the desired effect for unconnected precondition rules $pre(\cdot)_v$ where $v \in \mathbb{E}$. Maximum operation steps are set to terminate the search. Once the critical action is found, the critical action will be considered as the predecessor of previous critical actions.

DRL agent. In the training stage, we aim to train a DRL agent that can learn the subtask by leveraging the feature-extracting power of neural networks. The induction module only specifies the coarse-grained critical action to express temporal order. Therefore, the framework deploys DRL to complete the fine-grained decision-making tasks, which utilizes deep learning to approximate the optimal policy with neuron networks. DRL uses the policy gradient method to update the policy. In the proposed method, we use the action-critic method [38, 43] as the DRL agent. The implementation details are described in Appendix B.4.

Intrinsic rewards. During the training stage, if the agent successfully executes the critical effects, it will receive an intrinsic reward when the preconditions of a critical action ψ are satisfied. Conversely, if the agent takes an action that leads to undesired effects, such as violating effect rules, it will receive a penalty. However, note that our model only specifies positive critical actions and does not explicitly identify actions that have possible negative consequences. Therefore, the implementation of a penalty depends on the specific domain.

6 Experiments

We evaluate our framework and provide ablation studies in this section. Section 6.1 lists the algorithms we use for comparison. Section 6.2 provides the description of the environments and tasks. Section 6.3 presents the results of training efficiency and accuracy. Section 6.4 demonstrates the generalizability in different levels.

6.1 Baselines

We extensively compare our framework to various DRL algorithms (DQN and PPO) learning from *rewards*, imitation learning methods (BC and GAIL) learning from *demonstrations*, advanced approaches (DQN-RBS and BC-PPO) that leverage both *rewards* and *demonstrations*, and an exploration method (RIDE) that maximizes *intrinsic and extrinsic rewards*.

- **Deep Q-Network (DQN; [37])** is an off-policy deep Q-learning algorithm.
- **Proximal Policy Optimization (PPO; [46])** is a state-of-the-art on-policy DRL algorithm.
- **Behavior cloning (BC; [45])** imitates an expert by learning from demonstrations in a supervised manner.
- **Generative adversarial imitation learning (GAIL; [19])** mimics expert behaviors via learning a generative adversarial network whose generator is a policy.
- **DQN-RBS** initializes the replay buffer of DQN with demonstrations, allowing for a performance boost. This is inspired by the replay buffer spiking technique [30].
- **BC-PPO** pre-trains a policy with BC using demonstrations and then fine-tunes the policy with PPO using rewards, similar to Video PreTraining (VPT; [5]).
- **Rewarding impact-driven exploration (RIDE; [44])** is a DRL exploration method inspired by the intrinsic curiosity module [42].

6.2 Environments & Tasks

To evaluate the proposed framework and the baselines, we design three groups of tasks in a 8×8 gridworld environment, where an agent can move along four directions {up, down, left, right} and interact with objects. The tasks are described as follows. See Appendix C for more details.

SWITCH considers the combination lock scenario that turns on the switches in sequential order, representing as the states x_1, x_2, \dots, x_k in a chain, where $x_i \forall i \in k$ is the state that after turning on

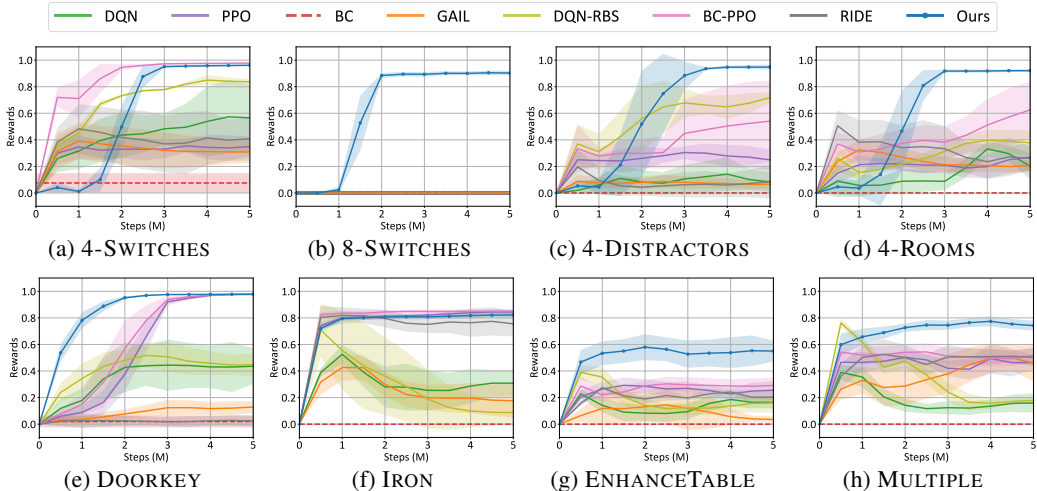


Figure 4: **Task performance.** We report the mean (line) and the standard deviation (shaded regions) of the training curves over 5M steps out of three runs. Our approach outperforms other methods, especially in advanced tasks.

switch i . If the wrong switch $j < i$ is toggled, the progress will reset to the previous state x_j . This configuration makes it challenging for DRL agents to solve the task solely through exploration. We design four tasks 4-SWITCH, 8-SWITCH, 4-DISTRACTORS and 4-ROOMS, where 4-SWITCH and 8-SWITCH evaluate the performance between different difficulties of tasks. 4-DISTRACTORS consist of four target switches and four distractor switches, and 4-ROOMS combines the configuration Minigrid *four-rooms* tasks [10].

DOORKEY features a hierarchical task similar to the Minigrid *door-key* tasks, where the agent needs to open a door with a key and turn on a switch behind the door.

MINECRAFT is inspired by the computer game Minecraft and is similar to the environment in previous works [50, 2, 55, 6]. The environment is designed for evaluation using multiple-task demonstrations. We select a simple task IRON, a difficult task ENHANCETABLE, and a multiple-goal task MULTIPLE.

For the methods that require demonstrations, we collect 20 demonstrations from corresponding tasks in SWITCH and DOORKEY and collect 64 multiple-task demonstrations from MULTIPLE for all tasks in MINECRAFT. More details about the environment and the tasks can be found in Appendix C.

6.3 Results

The experimental results in Figure 4 show that our framework outperforms all the baselines on challenging tasks (*e.g.*, 8-SWITCH, 4-DISTRACTORS, ENHANCETABLE, MULTIPLE) and performs competitively on simpler tasks (*e.g.*, DOORKEY, 4-SWITCHES, IRON). The imitation learning approaches, BC and GAIL, fail to learn all the tasks due to insufficient demonstrations and lack of exploration, while RIDE, BC-PPO, and DQN-RBS, which consider rewards online, fail on advanced tasks that require long-term planning. In contrast, our framework can leverage the knowledge from the same number of demonstrations and efficiently explore the environment, especially on the tasks 8-SWITCHES where all the baselines completely fail, as shown in Figure 4b. Moreover, our proposed framework is the most sample-efficient method in learning the DOORKEY task.

6.4 Generalizability

Our framework employs the critical-action model to achieve task-level generalizability, enabling the construction of novel task structures based on familiar critical actions. Additionally, we introduce genetic programming, renowned for its adaptability in reasoning symbolic rules as task substructures, thereby enhancing generalizability at the rule level. To define the domain gap, we denote the *original domain* as the domain where demonstrations are collected and the *variant domain* as the domain where agents learn. For rule-level generalizability, we define a variant critical action ϕ from ψ where $\mathcal{V}(eff(\phi)) = \mathcal{V}(eff(\psi))$ and $\mathcal{V}(pre(\phi)) = \mathcal{V}(pre(\psi))$ while $eff(\phi) \neq eff(\psi)$ or $pre(\phi) \neq pre(\psi)$. If a critical action ψ varies, the induced symbolic programs and the population can evolve and adapt to new substructures. Since $\mathcal{V}(pre(\phi))$ and $\mathcal{V}(eff(\phi))$ are known, the procedure starts from inducing effect rules $eff(\phi) \neq eff(\psi)$. Thus, the proposed framework can potentially achieve task generalization.

Setup. To evaluate the generalizability of our framework and baselines, we consider 4-SWITCHES-(N+1) as the original domain and its variant domains, 8-SWITCHES-(N+1), 4-DISTRACTORS-(N+1), and 4-DISTRACTORS-(2N+1). In 8-SWITCHES-(N+1), we extend the number of switches from 4 to 8 to evaluate the generalization of task structures. In 4-DISTRACTORS-(N+1), 4 distractor switches are added to 4-SWITCHES-(N+1). The order of switches in 4-DISTRACTORS-(2N+1) changes to $2n + 1$ (*e.g.*, $1 \rightarrow 3 \rightarrow 5 \rightarrow 7$), while the order of switches in 4-DISTRACTORS-(N+1) is $n + 1$ (*e.g.*, $1 \rightarrow 2 \rightarrow 3 \rightarrow 4$). This series of settings evaluates if a method can generalize to different effect rules. We collect 200 demonstrations in 4-SWITCHES-(N+1) and run 5M steps for all methods. For 4-DISTRACTORS-(2N+1), we collect *only* 4 additional demonstrations for all methods, and our framework leverages the previous populations of genetic programming to re-induce the rules, which only require few-shot demonstrations.

Table 1: **Generalization performance** in the original domain 4-SWITCHES and its variant domains.

Task	GAIL	BC-PPO	Ours
4-SWITCHES-(N+1)	30%±8%	97% ±0%	96% ±1%
8-SWITCHES-(N+1)	10%±2%	00%±0%	90% ±2%
4-DISTRACTORS-(N+1)	10%±7%	41%±4%	95% ±2%
4-DISTRACTORS-(2N+1)	11%±6%	33%±2%	95% ±1%

Baselines. We compare our framework with the best-performing baseline, BC-PPO, and the most widely used baseline, GAIL, for the generalization experiments.

Results. The results in Table 1 demonstrate that the performance of GAIL and BC-PPO drops in the variant domains, whereas our framework is able to generalize, highlighting its ability to construct novel rules and structures in the variant domains.

6.5 Ablation Study

This section presents the ablation studies of the induction modules. Section 6.5.1 qualitatively examines the mutual information and Section 6.5.2 shows the accuracy of symbolic regression using genetic programming.

6.5.1 Action-Effect Linkage

In Section 5.1, we introduce action-effect linkages to discover the co-occurred effect variables and actions. Figure 5 presents the experimental results in MINECRAFT and shows the relationship between the logarithm of mutual information and action-effect linkages. The heat map visualizes the values of mutual information of all action-effect pairs, with darker colors indicating higher values and stronger associations, highlighting the linkages. For instance, {wood, stick} is the effect variables of make_stick as mentioned in Figures 1a and 1b, discovered by our framework from executing make1. The results demonstrate a significant difference in mutual information between linked action and effect variables compared to unrelated ones.

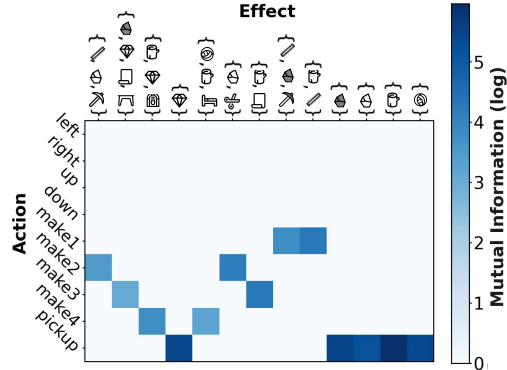


Figure 5: **Action-effect mutual information in MINECRAFT inferred by our framework.**

6.5.2 Symbolic Regression

The proposed framework necessitates a robust symbolic regression module to generate the symbolic rules. In Section 5.1, we introduce genetic programming as symbolic regression for induction. Since genetic programming is a randomized search method, empirical results are shown to discuss the success rate of finding correct rules and how much demonstrations are required to capture the symbolic rules.

The experiment setting is described as follows.

In MINECRAFT environment, there are 27 effect rules listed in Table 3. We sample different numbers of demonstrations from random subtasks, and the number of population are 500, 1000, and 2000. Other parameters of genetic programming are the same as the setting in Table 2. We calculate the number of programs which is equivalent to the ground truth after simplification. The result is the average accuracy out of five runs shown in Figure 6. We claim that the effect rules can be induced via genetic programming when a sufficient number of demonstrations and programs in the population are available. Noting that the results are related to the diversity of the data and its coverage of counterexamples relevant to the induction process. In addition, critical-action networks can still be built when some rules are inequivalent to the ground truth due to the bias of the data, as long as the rules match with the precondition of succeeding critical actions.

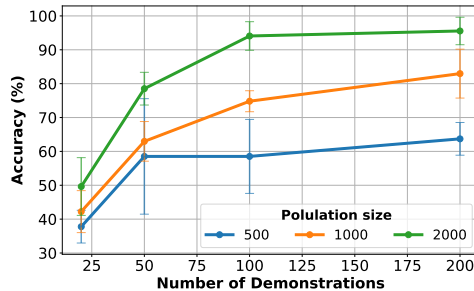


Figure 6: **Symbolic regression accuracy.**

7 Discussions

We presented a framework to address sparse-reward, goal-directed MDP tasks by integrating DRL and classical planning techniques. Our proposed framework represents symbolic knowledge as critical actions and employs a procedure to automatically extract knowledge from a few near-optimal

demonstrations. This combination of inductive learning (*i.e.*, DRL) and deductive learning (*i.e.*, classical planning) enables our framework to perform explicit high-level planning and accurate low-level execution, allowing for robust task performance and generalizing to unseen domains. Additionally, the proposed evolutionary computation provides adaptability at the rule level by inducing the task substructures. Under the mechanism, the agent can adapt to new environments by generating new symbolic knowledge from a pool of candidate programs.

Specifically, by representing knowledge as critical actions and employing critical-action networks, we provided a structured and organized mechanism for capturing and utilizing symbolic knowledge within DRL. The proposed procedures of subtask decomposition combine planning and DRL, leading to effective and efficient learning in goal-directed tasks. Furthermore, the compositionality of the critical-action model allows for different levels of generalization, and hence such a model has the potential to address a wide range of general problems. To sum up, our work offers a perspective to integrate inductive and deductive learning on general goal-directed decision-making problems.

This work extensively evaluates our proposed framework on deterministic, fully observable environments within the integer domain. To extend our proposed framework to complex domains, such as continuous input, we can potentially leverage recent studies that have developed genetic programming for different variable types [60, 61]. When facing stochastic or partially observable environments, the induction module can fail to induce some critical actions because of the uncertainty. In a worst-case scenario, when the induction module produces no rule, the proposed framework simply reduces to the backbone DRL algorithm (*i.e.*, PPO) without any intrinsic reward. One potential direction to address this issue is to extend the induction module to recognize and infer probabilistic rules [40, 3], which is left for future work.

8 Acknowledgement

The authors would like to thank the support of the National Science and Technology Council in Taiwan under grant No. NSTC 111-2221-E-002-189 and National Taiwan University under grant No. 112L891103. Shao-Hua Sun was partially supported by the Yushan Fellow Program by the Ministry of Education, Taiwan.

References

- [1] David Abel, Dilip Arumugam, Lucas Lehnert, and Michael Littman. State abstractions for lifelong reinforcement learning. In *International Conference on Machine Learning*, 2018.
- [2] Jacob Andreas, Dan Klein, and Sergey Levine. Modular multitask reinforcement learning with policy sketches. In *International Conference on Machine Learning*, 2017.
- [3] Ankuj Arora, Humbert Fiorino, Damien Pellier, Marc Métivier, and Sylvie Pesty. A review of learning planning action models. *The Knowledge Engineering Review*, 2018.
- [4] Kai Arulkumaran, Marc Peter Deisenroth, Miles Brundage, and Anil Anthony Bharath. Deep reinforcement learning: A brief survey. *IEEE Signal Processing Magazine*, 2017.
- [5] Bowen Baker, Ilge Akkaya, Peter Zhokov, Joost Huizinga, Jie Tang, Adrien Ecoffet, Brandon Houghton, Raul Sampedro, and Jeff Clune. Video pretraining (VPT): Learning to act by watching unlabeled online videos. In *Neural Information Processing Systems*, 2022.
- [6] Ethan Brooks, Janarthanan Rajendran, Richard Lewis, and Satinder Singh. Reinforcement learning of implicit and explicit control flow in instructions. In *International Conference on Machine Learning*, 2021.
- [7] Richard Byrne and Anne Russon. Learning by imitation: A hierarchical approach. *Behavioral and Brain Sciences*, 1998.
- [8] Christer Bäckström and Bernhard Nebel. Complexity results for SAS⁺ planning. *Computational Intelligence*, 1995.
- [9] Ethan Callanan, Rebecca De Venezia, Victoria Armstrong, Alison Paredes, Tathagata Chakraborti, and Christian Muise. MACQ: A holistic view of model acquisition techniques. In *The ICAPS Workshop on Knowledge Engineering for Planning and Scheduling*, 2022.
- [10] Maxime Chevalier-Boisvert, Bolun Dai, Mark Towers, Rodrigo de Lázcano, Lucas Willems, Salem Lahlou, Suman Pal, Pablo Samuel Castro, and Jordan Terry. Minigrad & mineworld: Modular & customizable reinforcement learning environments for goal-oriented tasks. *CoRR*, abs/2306.13831, 2023.
- [11] Luis Cobo, Peng Zang, Charles Isbell, and Andrea Thomaz. Automatic state abstraction from demonstration. In *International Joint Conference on Artificial Intelligence*, 2011.
- [12] Mohamad Hosein Danesh, Panpan Cai, and David Hsu. Leader: Learning attention over driving behaviors for planning under uncertainty. In *Conference on Robot Learning*, 2023.
- [13] Carlos Florensa, Yan Duan, and Pieter Abbeel. Stochastic neural networks for hierarchical reinforcement learning. In *International Conference on Learning Representations*, 2017.
- [14] Maria Fox and Derek Long. PDDL2.1: An extension to PDDL for expressing temporal planning domains. *Journal of Artificial Intelligence Research*, 2003.
- [15] Daniel Furelos-Blanco, Mark Law, Anders Jonsson, Krysia Broda, and Alessandra Russo. Induction and exploitation of subgoal automata for reinforcement learning. *Journal of Artificial Intelligence Research*, 2021.
- [16] Malik Ghallab, Craig Knoblock, David Wilkins, Anthony Barrett, Dave Christianson, Marc Friedman, Chung Kwok, Keith Golden, Scott Penberthy, David Smith, Ying Sun, and Daniel Weld. PDDL - the planning domain definition language. 1998.
- [17] Lin Guan, Sarath Sreedharan, and Subbarao Kambhampati. Leveraging approximate symbolic models for reinforcement learning via skill diversity. *arXiv preprint arXiv:2202.02886*, 2022.
- [18] Bradley Hayes and Brian Scassellati. Autonomously constructing hierarchical task networks for planning and human-robot collaboration. In *IEEE International Conference on Robotics and Automation*, 2016.

- [19] Jonathan Ho and Stefano Ermon. Generative adversarial imitation learning. *Advances in Neural Information Processing Systems*, 2016.
- [20] Rodrigo Toro Icarte, Ethan Waldie, Toryn Klassen, Rick Valenzano, Margarita Castro, and Sheila McIlraith. Learning reward machines for partially observable reinforcement learning. *Neural Information Processing Systems*, 2019.
- [21] Rodrigo Toro Icarte, Toryn Klassen, Richard Valenzano, and Sheila A. McIlraith. Reward machines: exploiting reward function structure in reinforcement learning. *Journal of Artificial Intelligence Research*, 2022.
- [22] Mu Jin, Zhihao Ma, Kebing Jin, Hankz Hankui Zhuo, Chen Chen, and Chao Yu. Creativity of ai: Automatic symbolic option discovery for facilitating deep reinforcement learning. In *AAAI Conference on Artificial Intelligence*, 2022.
- [23] B Ravi Kiran, Ibrahim Sobh, Victor Talpaert, Patrick Mannion, Ahmad A. Al Sallab, Senthil Yogamani, and Patrick Pérez. Deep reinforcement learning for autonomous driving: A survey. *IEEE Transactions on Intelligent Transportation Systems*, 2022.
- [24] George Konidaris, Leslie Pack Kaelbling, and Tomas Lozano-Perez. From skills to symbols: Learning symbolic representations for abstract high-level planning. *Journal of Artificial Intelligence Research*, 2018.
- [25] John Koza. Genetic programming: On the programming of computers by means of natural selection. *Statistics and computing*, 1994.
- [26] Tejas Kulkarni, Karthik Narasimhan, Ardavan Saeedi, and Joshua B. Tenenbaum. Hierarchical deep reinforcement learning: Integrating temporal abstraction and intrinsic motivation. *Advances in Neural Information Processing Systems*, 2016.
- [27] Junkyu Lee, Michael Katz, Don Joven Agravante, Miao Liu, Tim Klinger, Murray Campbell, Shirin Sohrabi, and Gerald Tesauro. AI planning annotation in reinforcement learning: Options and beyond. In *Planning and Reinforcement Learning Workshop at International Conference on Automated Planning and Scheduling*, 2021.
- [28] Youngwoon Lee, Shao-Hua Sun, Sriram Somasundaram, Edward Hu, and Joseph J. Lim. Composing complex skills by learning transition policies. In *International Conference on Learning Representations*, 2019.
- [29] Yu-An Lin, Chen-Tao Lee, Guan-Ting Liu, Pu-Jen Cheng, and Shao-Hua Sun. Addressing long-horizon tasks by integrating program synthesis and state machines. *arXiv:2311.15960*, 2023.
- [30] Zachary C Lipton, Jianfeng Gao, Lihong Li, Xiujun Li, Faisal Ahmed, and Li Deng. Efficient exploration for dialogue policy learning with bbq networks & replay buffer spiking. *arXiv preprint arXiv:1608.05081*, 2016.
- [31] Anthony Liu, Sungryull Sohn, Mahdi Qazwini, and Honglak Lee. Learning parameterized task structure for generalization to unseen entities. In *AAAI Conference on Artificial Intelligence*, 2022.
- [32] Guan-Ting Liu, En-Pei Hu, Pu-Jen Cheng, Hung-Yi Lee, and Shao-Hua Sun. Hierarchical programmatic reinforcement learning via learning to compose programs. In *International Conference on Machine Learning*, 2023.
- [33] Wei-Yin Loh. Classification and regression trees. *Wiley interdisciplinary reviews: data mining and knowledge discovery*, 2011.
- [34] Daoming Lyu, Fangkai Yang, Bo Liu, and Steven Gustafson. Sdrl: Interpretable and data-efficient deep reinforcement learning leveraging symbolic planning. In *AAAI Conference on Artificial Intelligence*, 2019.
- [35] Jiayuan Mao, Tomás Lozano-Pérez, Joshua B. Tenenbaum, and Leslie Pack Kaelbling. PDS-ketch: Integrated domain programming, learning, and planning. In *Neural Information Processing Systems*, 2022.

- [36] Volodymyr Mnih, Koray Kavukcuoglu, David Silver, Alex Graves, Ioannis Antonoglou, Daan Wierstra, and Martin Riedmiller. Playing atari with deep reinforcement learning. *arXiv preprint arXiv:1312.5602*, 2013.
- [37] Volodymyr Mnih, Koray Kavukcuoglu, David Silver, Andrei A Rusu, Joel Veness, Marc G Bellemare, Alex Graves, Martin Riedmiller, Andreas K Fidjeland, Georg Ostrovski, Stig Petersen, Charles Beattie, Amir Sadik, Ioannis Antonoglou, Helen King, Dhharshan Kumaran, Daan Wierstra, Shane Legg, and Demis Hassabis. Human-level control through deep reinforcement learning. *Nature*, 2015.
- [38] Volodymyr Mnih, Adria Puigdomenech Badia, Mehdi Mirza, Alex Graves, Timothy Lillicrap, Tim Harley, David Silver, and Koray Kavukcuoglu. Asynchronous methods for deep reinforcement learning. In *International Conference on Machine Learning*, 2016.
- [39] Thanh Thi Nguyen, Ngoc Duy Nguyen, and Saeid Nahavandi. Deep reinforcement learning for multiagent systems: A review of challenges, solutions, and applications. *IEEE Transactions on Cybernetics*, 2020.
- [40] Hanna Pasula, Luke Zettlemoyer, and Leslie Kaelbling. Learning symbolic models of stochastic domains. *Journal of Artificial Intelligence Research*, 2007.
- [41] Shubham Pateria, Budhitama Subagdja, Ah-hwee Tan, and Chai Quek. Hierarchical reinforcement learning: A comprehensive survey. *ACM Computing Surveys*, 2022.
- [42] Deepak Pathak, Pulkit Agrawal, Alexei A. Efros, and Trevor Darrell. Curiosity-driven exploration by self-supervised prediction. In *International Conference on Machine Learning*, 2017.
- [43] Antonin Raffin, Ashley Hill, Adam Gleave, Anssi Kanervisto, Maximilian Ernestus, and Noah Dormann. Stable-baselines3: Reliable reinforcement learning implementations. *Journal of Machine Learning Research*, 2021.
- [44] Roberta Raileanu and Tim Rocktäschel. RIDE: Rewarding impact-driven exploration for procedurally-generated environments. In *International Conference on Learning Representations*, 2020.
- [45] Stéphane Ross, Geoffrey Gordon, and Drew Bagnell. A reduction of imitation learning and structured prediction to no-regret online learning. In *International Conference on Artificial Intelligence and Statistics*, 2011.
- [46] John Schulman, Filip Wolski, Prafulla Dhariwal, Alec Radford, and Oleg Klimov. Proximal policy optimization algorithms. *arXiv preprint arXiv:1707.06347*, 2017.
- [47] Claude Elwood Shannon. A mathematical theory of communication. *The Bell system technical journal*, 1948.
- [48] Tom Silver and Rohan Chitnis. PDDL Gym: Gym environments from PDDL problems. In *Planning and Reinforcement Learning Workshop at International Conference on Automated Planning and Scheduling*, 2020.
- [49] Tom Silver, Ashay Athalye, Joshua B. Tenenbaum, Tomás Lozano-Pérez, and Leslie Pack Kaelbling. Learning neuro-symbolic skills for bilevel planning. In *Conference on Robot Learning*, 2022.
- [50] Sungryull Sohn, Junhyuk Oh, and Honglak Lee. Hierarchical reinforcement learning for zero-shot generalization with subtask dependencies. *Neural Information Processing Systems*, 2018.
- [51] Sungryull Sohn, Hyunjae Woo, Jongwook Choi, and Honglak Lee. Meta Reinforcement Learning with Autonomous Inference of Subtask Dependencies. *arXiv preprint arXiv:2001.00248*, 2020.
- [52] Sungryull Sohn, Hyunjae Woo, Jongwook Choi, Iyubing qiang, Izzeddin Gur, Aleksandra Faust, and Honglak Lee. Fast inference and transfer of compositional task structures for few-shot task generalization. In *Uncertainty in Artificial Intelligence*, 2022.

- [53] Roni Stern and Brendan Juba. Efficient, safe, and probably approximately complete learning of action models. In *International Joint Conference on Artificial Intelligence*, 2017.
- [54] Shao-Hua Sun, Hyeonwoo Noh, Sriram Somasundaram, and Joseph Lim. Neural program synthesis from diverse demonstration videos. In *International Conference on Machine Learning*, 2018.
- [55] Shao-Hua Sun, Te-Lin Wu, and Joseph J Lim. Program guided agent. In *International Conference on Learning Representations*, 2020.
- [56] Maxwell Svetlik, Matteo Leonetti, Jivko Sinapov, Rishi Shah, Nick Walker, and Peter Stone. Automatic curriculum graph generation for reinforcement learning agents. *AAAI Conference on Artificial Intelligence*, 2017.
- [57] Dweep Trivedi, Jesse Zhang, Shao-Hua Sun, and Joseph J Lim. Learning to synthesize programs as interpretable and generalizable policies. In *Neural Information Processing Systems*, 2021.
- [58] Mauro Vallati, Lukas Chrupa, Marek Grzes, Thomas Leo McCluskey, Mark Roberts, Scott Sanner, et al. The 2014 international planning competition: Progress and trends. *AI Magazine*, 2015.
- [59] Manuela Veloso, Jaime Carbonell, Alicia Perez, Daniel Borrajo, Eugene Fink, and Jim Blythe. Integrating planning and learning: The prodigy architecture. *Journal of Experimental & Theoretical Artificial Intelligence*, 1995.
- [60] Marco Virgolin, Tanja Alderliesten, Cees Witteveen, and Peter A. N. Bosman. Scalable genetic programming by gene-pool optimal mixing and input-space entropy-based building-block learning. In *Genetic and Evolutionary Computation Conference*, 2017.
- [61] Marco Virgolin, Tanja Alderliesten, Cees Witteveen, and Peter AN Bosman. Improving model-based genetic programming for symbolic regression of small expressions. *Evolutionary computation*, 29(2):211–237, 2021.
- [62] Lucas Willems. PyTorch Actor-Critic deep reinforcement learning algorithms: A2C and PPO. <https://github.com/lcswillems/torch-ac>, 2022.
- [63] Zhe Xu, Bo Wu, Aditya Ojha, Daniel Neider, and Ufuk Topcu. Active finite reward automaton inference and reinforcement learning using queries and counterexamples. In *Machine Learning and Knowledge Extraction*, 2021.
- [64] Qiang Yang, Kangheng Wu, and Yunfei Jiang. Learning action models from plan examples using weighted max-sat. *Artificial Intelligence*, 2007.

Appendix

A Preliminary Definition

This section provides the annotations of the Markov decision process (MDP) and planning specification discussed in Section 4. Section A.1 gives the formulation of MDP problems and Section A.2 explains the definition and the annotation of planning domain definition language (PDDL).

A.1 Markov Decision Process

A decision-making problem is formulated as a Markov decision process (MDP). MDP consists of a five-tuple $\langle \mathcal{S}, \mathcal{A}, T, R, \gamma \rangle$, where \mathcal{S} denotes state space, \mathcal{A} denotes action space, $T : \mathcal{S} \times \mathcal{A} \rightarrow \mathcal{S}$ denotes a transition function, $R : \mathcal{S} \times \mathcal{A} \rightarrow \mathbb{R}$ denotes a reward function, and $\gamma \in (0, 1]$ denotes a discounting factor.

In contrast with classical planning, problems in reinforcement learning represent the actions and the states with vectors of numeric values instead of literal conjunctions. A state in \mathcal{S} is a n -dimension vector s , where each entry $s_i, i \in \{1, 2, \dots, n\}$, represents the value of a numeric variable. In this work, we focus on goal-directed sparse-reward problems. That is, given an initial state, the objective is to find a policy to reach a desired goal state, and the agent only receives rewards when reaching the goal state.

A.2 Planning Domain Definition Language

PDDL is a language in first-order logic to describe the domains and the problems. A domain description includes the specification of objects, variables, and action models with preconditions and effects. A problem description includes an initial state and goal specification. These standard language specifications allow off-the-shelf planners to deduce the optimal action sequence of the goal.

For theory formalism, we follow the representation of SAS^+ . To distinguish with MDP state space \mathcal{S} , the state space in the planning domain are denoted as \mathcal{S}' . A SAS^+ task Π can be represented as a tuple $\langle \mathcal{V}, \mathcal{O}, s'_{init}, p'_{goal} \rangle$, where \mathcal{V} is a set of variables, and \mathcal{O} is a set of operators in the domain. A state $s' \in \mathcal{S}'$ in the planning domain is an assignment to \mathcal{V} , and $s'_v \in \mathbb{R}$ is the value assigned to the variable $v \in \mathcal{V}$ in s' . $p' \subset s'$ is a partial state of s' , where p' is the assignment to $\mathcal{V}(p') \subset \mathcal{V}$. Specifically, $s'_{init} \in \mathcal{S}'$ is the initial state, and p'_{goal} is a partial state of the goal specification.

A logical condition l_v describes the relation between the variable v and an distinct value (e.g., $wood = 1, stick \geq 2$). Each operator $o \in \mathcal{O}$ can be described as an action schema in a pair $\langle pre(o), eff(o) \rangle$, where $pre(o)$ is a conjunction of logical conditions denoted the precondition needed to be satisfied before executing o , $eff(o)$ is a set of functions denoted the change toward the state variables after executing o . The prevail condition is a subset of $pre(o)$ which holds during the action and does not affect by the effect, denoted as $prv(o) = \{l_v \mid l_v \in pre(o), v \notin \mathcal{V}(eff(o))\}$. An operator o is admissible in state s' iff $pre(o) \subset s'$ and $prv(o) \subset s'$.

B Implementation Detail

In this section, we elaborate on the implementation detail of the proposed framework that was used in the experiments. We implement several modules using off-the-shelf packages and approaches, including genetic programming as symbolic regression with *gplearn*, the agents with PPO, and the intrinsic reward function we use in the experiments.

B.1 Algorithm in Extracting Action-Effect Linkages

In Algorithm 1, for each MDP action, we calculate the mutual information between the action and all combinations of effect variables in demonstrations. Then, we apply the two-center clustering method to determine the threshold shown in Algorithm 2. Two-center clustering finds a threshold value that separates a given data into two clusters, which minimizes the sum of distances of data points from their respective cluster centers. We take the logarithm of mutual information as the metric to avoid incorrect thresholds caused by extremely high mutual information.

Algorithm 1 Extracting Action-Effect Linkages

Input: Demonstrations, action set \mathcal{A} , effect set \mathcal{E} **Output:** Action-effect pairs with linkages L

```
 $L \leftarrow \emptyset$ 
for  $a$  in  $\mathcal{A}$  do
   $N_a \leftarrow \emptyset$ 
  for  $\mathcal{V}(\text{eff}(\cdot))$  in  $\mathcal{E}$  do
     $N_a \leftarrow N_a \cup M_{(a, \mathcal{V}(\text{eff}(\cdot)))}$ 
  end for
   $t \leftarrow \text{Two-Center-Clustering}(N_a)$ 
  for  $\mathcal{V}(\text{eff}(\cdot))$  in  $\mathcal{E}$  do
    if  $M_{(a, \mathcal{V}(\text{eff}(\cdot)))} \geq t$  then
       $L \leftarrow L \cup (a, \mathcal{V}(\text{eff}(\cdot)))$ 
    end if
  end for
end for
```

Algorithm 2 Two-Center-Clustering

Input: Data D with length n **Output:** Threshold of two clusters

```
 $cluster_1, cluster_2 \leftarrow \emptyset$ 
 $c_1, c_2 \leftarrow \min(D), \max(D)$ 
if  $c_1 = c_2$  then
  return  $c_1$ 
end if
 $terminated \leftarrow False$ 
while not  $terminated$  do:
  for  $i = 1$  to  $n$  do
    if  $|D[i] - c_1| < |D[i] - c_2|$  then
       $cluster_1 \leftarrow D[i]$ 
    else
       $cluster_2 \leftarrow D[i]$ 
    end if
  end for
   $c'_1, c'_2 \leftarrow \text{mean}(cluster_1), \text{mean}(cluster_2)$ 
  if  $c_1 = c'_1$  and  $c_2 = c'_2$  then
     $terminated \leftarrow True$ 
  end if
   $c_1, c_2 \leftarrow c'_1, c'_2$ 
end while
return  $(c_1 + c_2)/2$ 
```

B.2 Genetic Programming

Genetic programming is employed as a symbolic regressor for determining symbolic effect rules in the proposed methods, illustrated in Figure 3a. We use the *gplearn* package for implementation and the parameter settings of are shown in Table 2. Given the action-effect linkage $(a, \mathcal{V}(\text{eff}(\cdot)))$, the transitions with action a are selected as the training data. For each effect variable v in $\mathcal{V}(\text{eff}(\cdot))$, the algorithm’s objective is to find the program $\text{eff}(\cdot)_v$ that predicts v after executing the action with the highest accuracy.

Each program is represented as an expression tree where input is the current state in the transition and output is the predicted value. The algorithm comprises several steps: initialization, evaluation, selection, crossover, and mutation. Initially, the population, which is a set of programs, is randomly generated. Fitness evaluation is then performed on all programs; a subset of programs with the highest fitness values is selected. These programs serve as parents to produce offspring through crossover and mutation mechanisms. Through iterative selection and production, the evolution of

Table 2: **The parameter setting of *gplearn*.** The parameter with two values indicates that the settings are different in two phases.

Parameters	Value (first/second phase)
population_size	2000/2000
tournament_size	40/40
generations	20/10
p_crossover	0.6/0.6
p_subtree_mutation	0.2/0.2
p_hoist_mutation	0.1/0.1
p_point_mutation	0.05/0.05
max_samples	0.95/0.95
init_depth	(2,6)/(2,6)
parsimony_coefficient	0.0001/0.005
function_set	{+, -, ×, ÷, inc, dec}/{+, -, ×, ÷, inc, dec}

the population to discover the programs that best fit the given data. The evaluation metric used in genetic programming is the percentage of correct effect prediction shown below:

$$fitness(eff(\cdot)_v) = \frac{\# \text{ of transitions with } (a, \mathcal{V}(eff(\cdot))) \text{ consistent with } eff(\cdot)_v}{\# \text{ of transitions with } (a, \mathcal{V}(eff(\cdot)))}, \quad (2)$$

where a transition consistent with $eff(\cdot)_v$ means that the predicted effect value $eff(\cdot)_v(s_v)$ is consistent with the actual one $T(s, a)$ given the transition $\langle s, a, T(s, a) \rangle$. To prevent bloat issues in which the program grows extremely large to fit the data, the algorithm contains two phases: exploring and pruning. The best programs with the highest accuracy are determined in the exploring phase. Subsequently, in the pruning phase, we set high parsimony to prune the program.

B.3 Decision Tree Method

The proposed framework uses classification and regression tree (CART) [33] to build decision trees. CART is a supervised learning algorithm that generates binary trees by recursive partitioning, where each internal node represents a decision based on a specific variable, and each leaf node represents a prediction. Let data partitioned at the internal node m denoted as D_m with n_m samples. The algorithm aims to find a decision with a variable q and a threshold t to partition D_m into two subsets D_m^0 and D_m^1 with n_m^0 and n_m^1 samples. The loss function of the partition is defined as follows:

$$G(D_m, q, t) = \frac{n_m^0}{n_m} H(D_m^0) + \frac{n_m^1}{n_m} H(D_m^1), \quad (3)$$

where $H(D_m^i)$ is the entropy of D_m^i . In each partition, the algorithm’s objective is to find the (q, t) that minimizes $G(D_m, q, t)$ at node m . This process is repeated until a stopping criterion is met.

In the given transition $\langle s, a, T(s, a) \rangle$ with a in demonstrations, the current states s are taken as inputs to a decision tree, and the outcome of the decision tree is a true value that whether $T(s, a)$ consistent with the rules in $eff(\cdot)$. After generating a decision tree by CART, the model of this decision tree is then transferred into a conjunction of rules by logical simplification and set as the precondition rules $pre(\cdot)$, while $\mathcal{V}(pre(\cdot))$ is the set of variables mentioned in $pre(\cdot)$. Considering the precondition is the conjunction of the precondition rules while the formula of the decision tree may involve disjunction, the decision tree model is transferred into the disjunctive normal form. Each clause in the disjunctive normal form is considered the precondition for different critical actions.

B.4 Deep Reinforcement Learning Module

In our research, we adopt the Proximal Policy Optimization (PPO) as the foundation for our framework and the baseline in this work, utilizing the *torch-ac* library [62] for implementation. The architecture of our model is designed to encode an 8x8 gridworld and state information.

The gridworld is handled by a convolutional neural network (CNN) comprising four layers. The network effectively processes the input images, which are formatted in a three-channel setup, representing the object, color, and status respectively. The first convolutional layer utilizes 32 filters with a kernel size of 3×3 and a stride of 2×2 . Subsequent layers employ 2×2 kernels, with channel sizes incrementing through 64, 96, to 128. Each layer integrates the ReLU activation function.

Parallely, the state representation, converted into PDDL, is encoded through a two-layer fully-connected network. Each of these layers contains 64 neurons and leverages the ReLU activation function for non-linear transformation.

Two types of encoded observation are concatenated and encoded by another two-layer 64×64 fully-connected network. The output-encoded observation is then used as the input of the actor network and the critic network. Both the encoding networks and the actor-critic networks are trained.

B.5 Reward Function

During the training stage, we train an agent with intrinsic rewards generated from the critical action network. The modified rewards function is illustrated as follows:

$$R_{int}(s) = \begin{cases} +1 & \text{if execute a critical action,} \\ 0 & \text{otherwise.} \end{cases} \quad (4)$$

Given the original reward function R as extrinsic rewards, the overall reward of the MDP problem is $R_{mod}(s) = R(s) + R_{int}(s)$. In the experiment, the reward function is defined as

$$R = \begin{cases} \frac{step_{max} - step}{step_{max}} & \text{if the episode terminated,} \\ 0 & \text{otherwise,} \end{cases} \quad (5)$$

where $step_{max}$ is the maximum number of steps in the environment, and $step$ is where $step$ is the current number of steps the agent has done. The setting of the maximum number of steps in each environment is described in Appendix C.

C Test Environments

We use three MDP environments: SWITCH, DOORKEY, and MINECRAFT for evaluation. The first environment SWITCH tests the ability to achieve sequential tasks. The second environment DOORKEY is similar to *door-key* in *Minigrid* which is a baseline environment with hierarchical tasks. The third environment MINECRAFT is designed to evaluate the ability to construct various task structures with multiple subtasks for compositional tasks. The following sections provide a description of the environments. The maximum number of steps in DOORKEY is 1600, while in SWITCH and MINECRAFT is 25600.

C.1 SWITCH

The environment SWITCH is designed to evaluate the ability to solve hierarchical tasks. In SWITCH, several switches are placed on the grid. The objective of the agent in SWITCH is to sequentially turn on switches in a pre-determined order.

We define the state variables as $\mathcal{V} = \{\text{at_switch}, \text{next_switch}, \text{goal_switch}\}$. `at_switch` indicates the switch the agent stays at. If the agent does not stay at any switch, this variable is set to zero. `next_switch` indicates which switch should be activated in the following actions. `goal_switch` denotes the last switch and also implies how many switches should be turned on. The action space \mathcal{A} contains five actions: `{left, right, up, down, toggle}`. `toggle` enables the agent to activate or deactivate a switch.

The switches have three states, including *available*, *on* and *off*. The agent can turn the *available* switch to *on*. If the agent executes the action `toggle` at the switch, it will be deactivated and turned to *available*. The agent can not change the status of the *off* switch until the predecessor switch is *on*. If a *on* switch is turned to *available*, all subsequent switches will also be deactivated. This makes it challenging for RL agents to solve the task through random walks or exploration alone.

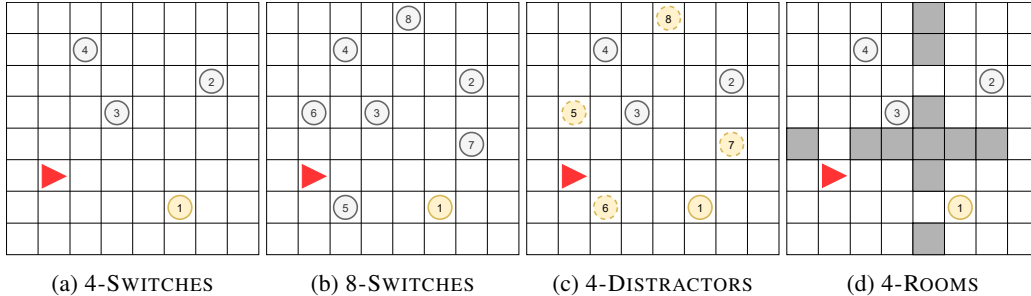


Figure 7: **Visualization of SWITCH environments.** N -SWITCHES in (a) and (b) shows the tasks which consist of 4 and 8 switches in incremental order. (c) N -DISTRACTORS is the variant N -SWITCHES with other n distractor switches (the circle with dotted line). (d) combines *four-room* environment in *Minigrid*, testing the navigation ability of the agent.

For various evaluations, we design several situations, including the number of switches, sequential order, and distractors. In the following sections, the settings of the tasks are listed and the illustrations can be found in Figure 7.

- **N -SWITCHES.** When the number of switches increases, the tasks become more difficult as it has more chance to turn off the switch. This setting evaluates the performance of different difficulties of tasks.
- **N -DISTRACTORS.** *Available* switches are added as distractors to the environment. The agent can turn on and off the distractor switches, but it does not help to achieve the tasks. In n -switch incremental-order tasks, the switches labeled $n + 1$ to $2n$ are set as distractors, while in n -switch incremental-order tasks, the switches labeled $2, 4, \dots, 2n$ are set as distractors. This setting evaluates whether the agent acquires the ability to select correct switches and neglects the incorrect ones.
- **4-ROOMS.** Two lines of walls divide the gridworld into four rooms according to the four-room configuration in *Minigrid*. Every two rooms are interconnected by a gap in the walls. In this scenario, the agent must navigate through the rooms considering the walls to activate the switches. This setting evaluates the efficacy of DRL involving navigating obstacles at low-level execution.
- **Order of the switches.** To evaluate generalizability, we define two types of orders including $(N+1)$ and $(2N+1)$. $(N+1)$ indicates that the switches should be turned on in incremental order (*i.e.*, $1 \rightarrow 2 \rightarrow 3 \rightarrow 4 \dots$) where ($\text{goal_switch} = n$), and $(2N+1)$ indicates that the switches should be turned on in odd order (*i.e.*, $1 \rightarrow 3 \rightarrow 5 \rightarrow 7 \dots$) where ($\text{goal_switch} = 2n + 1$). The order are labeled after the task name (*e.g.*, 4-DISTRACTORS- $(N+1)$), and by default the order is $(N+1)$.

C.2 DOORKEY

The environment DOORKEY presents a task where an agent must collect a key to unlock a door and turn on the switch behind the door. It is a basic setting which can be used to evaluate the ability to solve hierarchical tasks.

We define the state variables as $\mathcal{V} = \{\text{agent_dir}, \text{has_key}, \text{door_state}, \text{at_switch}, \text{at_door}, \text{next_switch}\}$. `agent_dir` indicates the agent direction, `has_key` indicates whether the agent holds the key, and `door_state` indicates the state of the door, including open, closed, and locked. The action space \mathcal{A} contains seven actions: `{left, right, up, down, toggle, pickup, drop}`. `toggle` enables the agent to activate a switch or open the door.

C.3 Minecraft

MINECRAFT is inspired by the computer game *Minecraft* and is similar to the environment in previous works [50, 2, 55, 6] illustrated in Figure 8a. The agent can pick up the primary materials on the map and make different tools in specific places consuming the materials. The

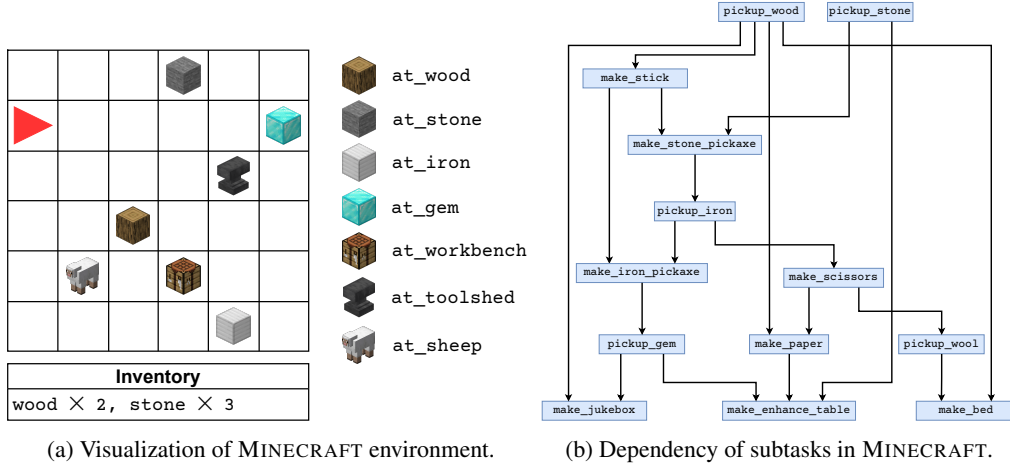


Figure 8: **Illustration of configuration and subtask dependencies in MINECRAFT environment.** (a) There are 7 locations in MINECRAFT environment, and the agent needs to collect materials and craft tools at specific location. (b) illustrate the dependencies of the critical actions. For instance, to execute pickup_iron, the agent needs to make a stone pickaxe. The graph ignores preconditions, effects, and the number of executions required.

goal of each task is to acquire the desired materials or tools. The state variables include $\{x, y, at_ < place >, < inventory >\}$, where $at_ < place >$ denotes whether the agent is at the place, and $< inventory >$ denotes the number of materials or tools the agent holds.

In our experiments, thirteen types of items are designed in the inventory: wood, stone, stick, iron, gen, stone_pickaxe, iron_pickaxe, wool, paper, scissors, bed, jukebox, enhance_table, and there are seven places on the grid world: at_wood, at_stone, at_iron, at_gem, at_sheep, at_workbench, at_toolshed.

The action space \mathcal{A} contains eight actions: $\{left, right, up, down, make1, make2, make3, make4\}$. The agent crafts different items when executing different make actions (make1, make2, make3, make4) and at different places (workbench or toolshed). The formulas of the items are listed in Table 3, and the dependency of the subtasks is illustrated in Figure 8b. The agent needs to get the materials to create desired items. We test two single tasks with different difficulties IRON and ENHANCETABLE, and a multiple task MULTIPLE that sample the goal at random.

Table 3: Formulas in MINECRAFT environment. The MDP actions, preconditions and effects are the same as their corresponding critical actions.

Inventory	MDP Action	Preconditions	Effects
wood	pickup	at_wood = 1 wood + 1	
stone	pickup	at_stone = 1 stone + 1	
iron	pickup	at_iron = 1 iron + 1	stone_pickaxe \geq 1
gem	pickup	at_gem = 1 gem + 1	iron_pickaxe \geq 1
wool	pickup	at_sheep = 1 wool + 1	scissors \geq 1
stick	make1	at_workbench = 1 stick + 1	wood - 1
stone_pickaxe	make1	at_toolshed = 1 stone_pickaxe + 1	stone - 3 stick - 2
iron_pickaxe	make2	at_toolshed = 1 iron_pickaxe + 1	iron - 3 stick - 2
iscissors	make2	at_workbench = 1 scissors + 1	iron - 2
paper	make3	at_workbench = 1 paper - 1	scissors \geq 1 wood - 1
bed	make3	at_toolshed = 1 bed + 1	wood - 3 wool - 3
jukebox	make4	at_workbench = 1 jukebox + 1	wood - 3 gem - 1
enhance_table	make4	at_toolshed = 1 enhance_table + 1	stone - 1 paper - 2 gem - 1

D Critical Action

The critical action and its graph are shown in this section. Tables 4 and 5 show the critical actions in DOORKEY and SWITCH environments. The rules of critical actions in MINECRAFT environment are already listed in Table 3 and are omitted in this section. Figures 9, 10, 11 and 12 illustrate the critical action networks of N-SWITCHES, DOORKEY, IRON and ENHANCETABLE, respectively.

Table 4: Critical actions in SWITCH environment.

Action Name	MDP Action	Preconditions	Effects
turn_on	toggle	at_switch = next_switch next_switch + 1	

Table 5: Critical actions in DOORKEY environment.

Action Name	MDP Action	Preconditions	Effects
pickup_key	pickup	at_key = 1 at_key = 0	has_key = 1
open_door	toggle	door_state = 0 door_state = 2	at_door = 1 agent_dir = 1
turn_on	toggle	at_switch = 1 next_switch + 1	door_state = 2

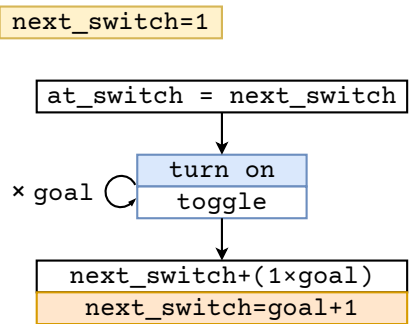


Figure 9: Critical action network of SWITCH

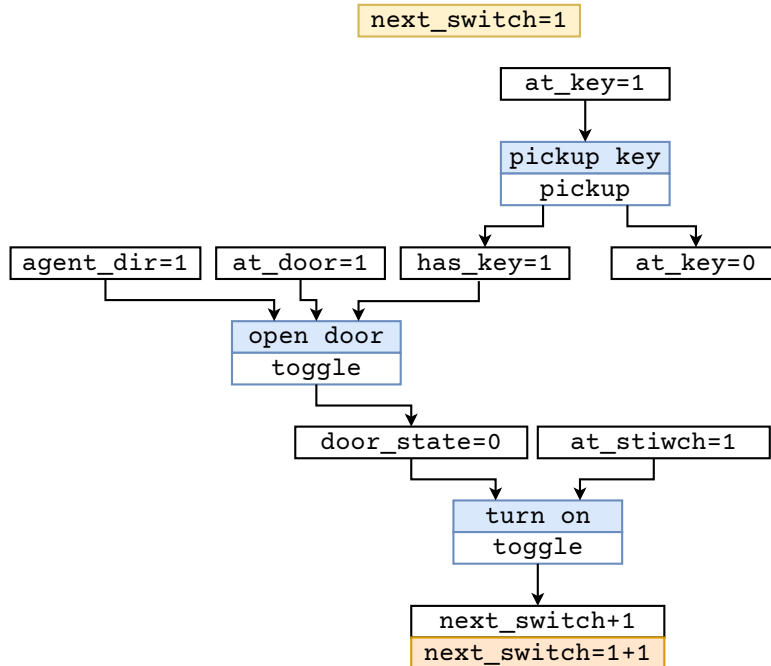


Figure 10: Critical action network of DOORKEY

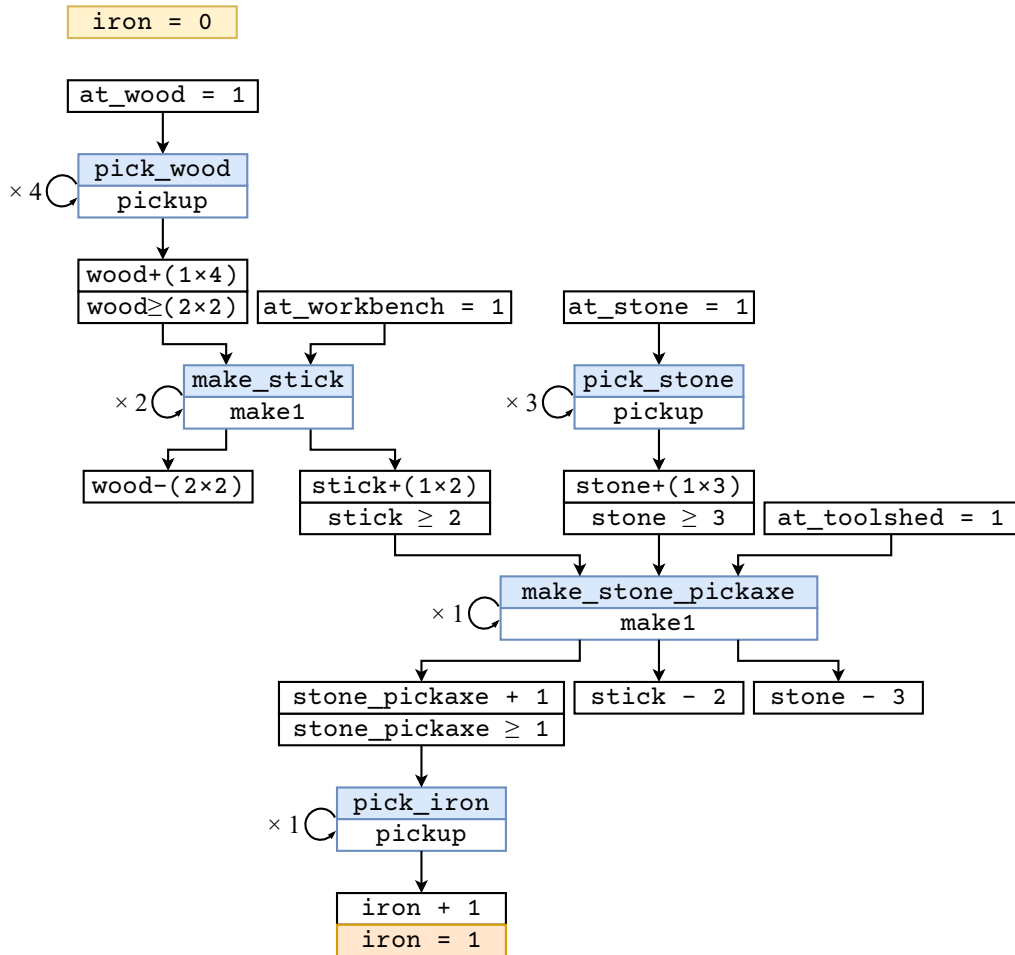


Figure 11: Critical action network of IRON

enhance_table = 0

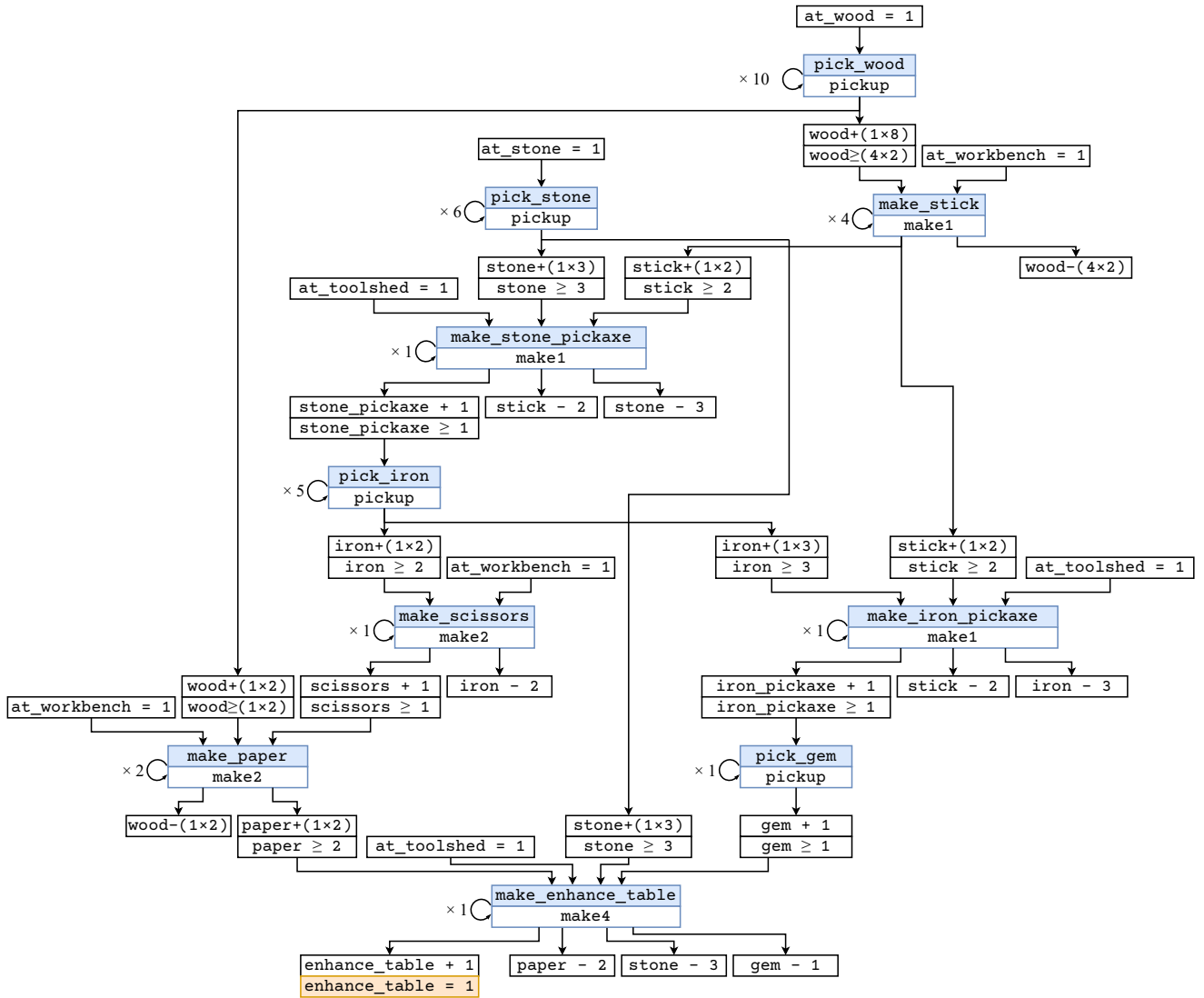


Figure 12: Critical action network of ENHANCETABLE